

Modulation of a pacemaker current through Ca^{2+} -induced stimulation of cAMP production

Anita Lüthi and David A. McCormick

Yale University School of Medicine, Section of Neurobiology, 333 Cedar Street, New Haven, Connecticut 06510, USA

Correspondence should be addressed to D.A.M. (mccormick@biomed.med.yale.edu)

Brief increases in $[\text{Ca}^{2+}]_i$ can result in prolonged changes in neuronal properties. A Ca^{2+} -dependent modulation of the hyperpolarization-activated cation current (I_h) controls the slow recurrence of synchronized thalamocortical activity. Here we show that the persistent activation of I_h is initiated by rapidly increased $[\text{Ca}^{2+}]_i$ and subsequent production of cAMP. The modulation is maintained via a facilitated interaction of cAMP with open (voltage-gated) h-channels, inducing prolonged activation of I_h that may outlast the presence of increased free $[\text{Ca}^{2+}]_i$ and $[\text{cAMP}]_i$. This persistent I_h activation may control the presence and periodicity of both normal and abnormal synchronized thalamocortical rhythms.

Activity-induced transient increases in intracellular Ca^{2+} concentration ($[\text{Ca}^{2+}]_i$) trigger neuronal responses ranging from modulation of synaptic transmission to alterations in gene expression with time courses of seconds to days^{1–3}. These changes occur through Ca^{2+} -stimulated messenger cascades that can induce prolonged recruitment of proteins by, for example, autophosphorylation⁴, persistent binding to Ca^{2+} /calmodulin⁵ or transcription factor activation⁶.

Increased $[\text{Ca}^{2+}]_i$ may also affect the intrinsic electrical characteristics of neurons by modifying properties of ionic channels⁷, through, for example, Ca^{2+} -triggered activation of kinases or adenylyl cyclases. However, because few studies (for example, ref. 8) have quantitatively investigated the temporal relationship between activity-dependent $[\text{Ca}^{2+}]_i$ elevation and its effects on ionic conductances in intact central neurons, how much these modulations may contribute to persistent changes in neuronal circuits is unclear.

Hyperpolarization-activated cation currents (I_h) are widely expressed in the nervous system and often function as ‘pacemaker’ currents for rhythmic electrical behavior^{9–11}. The role of I_h is well characterized in thalamocortical cells, where this current not only contributes to rhythmic discharges of single neurons, but also governs the slow periodic recurrence of network activities^{10–13}. Thalamic synchronized oscillations in the form of spindle waves appear as 1–4-second periods of synchronized activity interspersed by silent phases of 5–20 seconds¹⁴. The oscillatory period arises as a cyclical interaction between thalamocortical cells and inhibitory neurons from the nucleus reticularis thalami (nRT) or perigeniculate nucleus (PGN)¹⁵. Burst firing in nRT/PGN neurons induces rhythmic IPSPs in thalamocortical cells, which, in turn, generate rebound low-threshold Ca^{2+} spikes and bursts of action potentials that re-excite the nRT/PGN neurons.

The silent period between spindle waves is largely determined by persistent I_h activation in thalamocortical cells^{12,13,16}. This activation, initiated during the oscillatory period, causes thalamo-

cortical cells to generate a slowly decaying (tens of seconds) afterdepolarization (ADP)¹² that prevents the generation of rebound bursts, thereby stopping the oscillations. This persistent I_h activation is induced partly by transient $[\text{Ca}^{2+}]_i$ increases resulting from rebound Ca^{2+} spikes during the oscillations¹⁶. Although the time course of the silent period between these oscillations *in vitro* is largely controlled by the slow decay of the ADP^{12,13}, what determines the temporal dynamics of persistent I_h activation remains unclear. Here we show that I_h enters a state of Ca^{2+} -independent persistent activation via allosterically stabilized interaction with cAMP released upon Ca^{2+} entry, thus indicating a direct relationship between ionic channel function and slow network activity¹⁰.

RESULTS

Time course of Ca^{2+} -mediated upregulation of I_h

To assess modulation of I_h by increases in $[\text{Ca}^{2+}]_i$, we applied 20 hyperpolarizing current pulses (4 Hz, 125 ms, 500 pA), each large enough to evoke a low-threshold Ca^{2+} spike, to thalamocortical cells using whole-cell patch-clamp recordings. This protocol, which partially mimics the events occurring during synchronized network oscillations in thalamocortical cells^{12,16}, reliably enhanced I_h . Thus, these injections were followed by a small, slowly decaying ADP (Fig. 1a; 2–6 mV) that was abolished by extracellular application of Cs^+ (2–5 mM in bath; $n = 4$; data not shown), an I_h blocker^{9,11}. I_h amplitude was measured in voltage-clamp conditions after the end of the current injections. At ADP peak (1–2 s after current pulses), I_h was significantly increased to $142 \pm 14\%$ of control (test potential -78 mV; $n = 5$; $p < 0.05$) and decayed monoexponentially with a time constant of $\tau = 12.8 \pm 1.3$ s, matching the slow decay of the ADP (Fig. 1a–c; $n = 5$).

Upregulation of I_h was also observed following UV-flash-induced photolytic release of caged Ca^{2+} perfused into the cytosol and was characterized by a transient, reversible enhancement of the amplitude of I_h responses¹⁶ (Fig. 1d and e; $114 \pm 1.3\%$ of control in 22 of 32 cells; range 105–126%; $p < 0.0001$). The size of

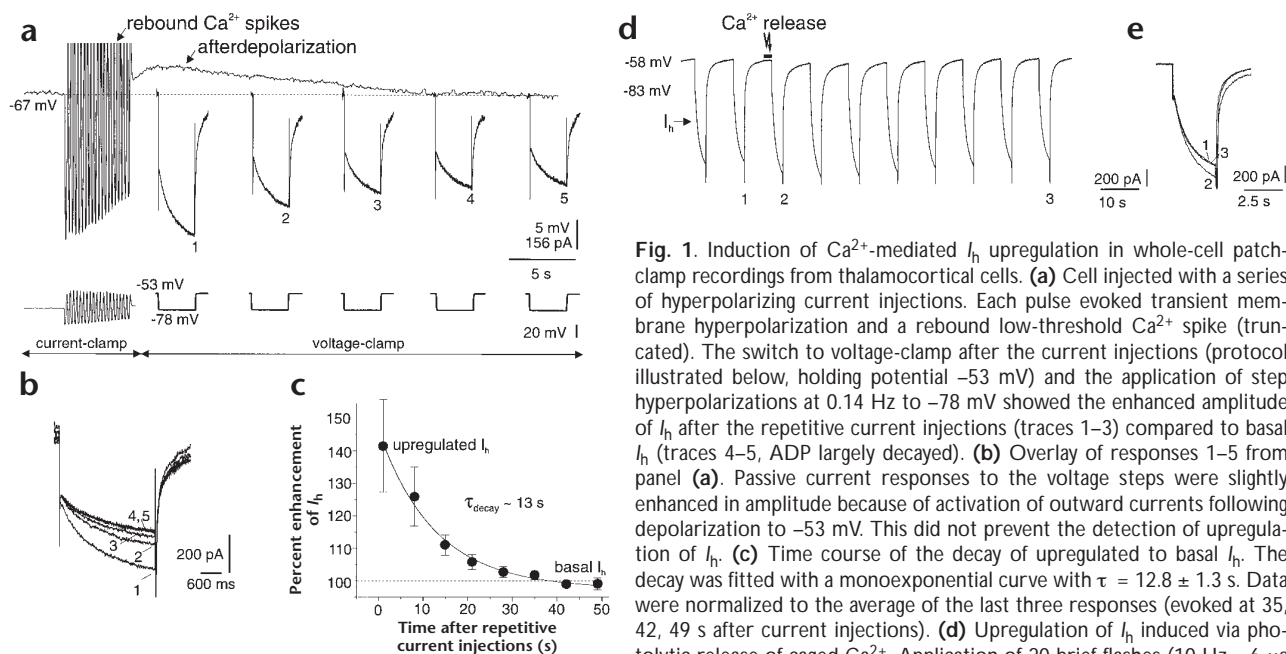


Fig. 1. Induction of Ca^{2+} -mediated I_h upregulation in whole-cell patch-clamp recordings from thalamocortical cells. **(a)** Cell injected with a series of hyperpolarizing current injections. Each pulse evoked transient membrane hyperpolarization and a rebound low-threshold Ca^{2+} spike (truncated). The switch to voltage-clamp after the current injections (protocol illustrated below, holding potential -53 mV) and the application of step hyperpolarizations at 0.14 Hz to -78 mV showed the enhanced amplitude of I_h after the repetitive current injections (traces 1–3) compared to basal I_h (traces 4–5, ADP largely decayed). **(b)** Overlay of responses 1–5 from panel **(a)**. Passive current responses to the voltage steps were slightly enhanced in amplitude because of activation of outward currents following depolarization to -53 mV. This did not prevent the detection of upregulation of I_h . **(c)** Time course of the decay of upregulated to basal I_h . The decay was fitted with a monoexponential curve with $\tau = 12.8 \pm 1.3$ s. Data were normalized to the average of the last three responses (evoked at 35, 42, 49 s after current injections). **(d)** Upregulation of I_h induced via photolytic release of caged Ca^{2+} . Application of 20 brief flashes (10 Hz, ~ 6 μs each, marked by black bar) induced a reversible enhancement of the amplitude of I_h (arrow). **(e)** Overlay of responses 1–3 from **(d)**.

this increase was correlated with that evoked by Ca^{2+} entry through voltage-gated channels; cells showing large ADPs following repetitive hyperpolarization (> 4 mV) gave the largest responses to Ca^{2+} release ($117.5 \pm 3.0\%$ at -83 mV; $n = 4$), whereas cells showing small ADPs (< 3 mV) gave small responses ($105.6 \pm 2.0\%$ at -83 mV; $n = 5$). Also, I_h enhancement induced via photolytic Ca^{2+} release was strongest in the middle of the I_h activation range (-65 to -95 mV), indicating a shift in I_h voltage dependence, as shown for Ca^{2+} entering through voltage-gated channels¹⁶.

cAMP occludes Ca^{2+} effects on I_h

The slow time course of Ca^{2+} -induced upregulation of I_h suggests an indirect effect of Ca^{2+} (for example, via production of second messengers such as cyclic nucleotides^{9,16}). We therefore examined the effects of simultaneous exposure of I_h to cAMP and Ca^{2+} . Cyclic AMP (10–1000 μM in the patch pipet) caused a dose-dependent positive shift of the I_h activation curve^{9,11,17,18}. The half-activation voltage (V_{50}) was determined by fitting the Boltzman equation, $I/I_{\text{max}} = \{1 + \exp[(V_m - V_{50})/s]\}^{-1}$, to normalized activation curves (Fig. 2a). Control I_h yielded $V_{50} = -83.6 \pm 0.5$ mV and $s = 6.9 \pm 0.2$ mV ($n = 16$)¹⁹. The shift in V_{50} varied with cAMP concentration in a sigmoidal concentration-response curve that was fit with the Hill equation $y/y_{\text{max}} = \{1 + (c/c_0)^p\}^{-1}$ (Fig. 2e). This yielded values of 9.15 ± 1.0 mV for the maximal effect y_{max} , 45.5 ± 7.1 μM for the half-maximal concentration c_0 and -2.5 ± 0.8 for the Hill coefficient p ($n = 3$ –5 cells for each data point). In parallel, cAMP dose-dependently reduced the ADP (following a saturating number of hyperpolarizing current injections, Fig. 2c). This was well described by the Hill equation, with $y_{\text{max}} = 4.5 \pm 0.5$ mV, $c_0 = 39.0 \pm 6.9$ μM and $p = 1.1 \pm 0.2$ (Fig. 2e; $n = 3$ –7 cells for each data point). Thus, V_{50} shifts for I_h activation and ADP occlusion similarly depended on cAMP concentration, with $c_0 \approx 40$ μM . This concentration is about two orders of magnitude

higher than that reported in a cell-free system¹⁷, presumably reflecting hydrolysis of cAMP perfused through the pipet. Therefore, cAMP experiments were repeated with the non-hydrolyzable analog 8BrcAMP, which induced a dose-dependent occlusion of the ADP with $y_{\text{max}} = 4.5 \pm 0.29$ mV, $c_0 = 0.36 \pm 0.04$ μM and $p = 1.29 \pm 0.19$ (Fig. 2d and e; $n = 3$ –7 per data point), thus showing ~ 100 -fold higher potency than cAMP. Similarly, the activation curve shift was characterized by $y_{\text{max}} = 10.4 \pm 1.2$ mV, $c_0 = 0.18 \pm 0.04$ μM and $p = -0.77 \pm 0.11$ (Fig. 2b and e; $n = 3$ –7 cells for each data point). These values closely agree with data obtained from application of cAMP to inside-out patches ($c_0 = 0.21$ μM , $p = -0.85$)¹⁷. The reciprocal correlation in the concentration dependence of the V_{50} shift and the ADP occlusion, along with the low Hill coefficient (~ 1 for 8BrcAMP), suggests that Ca^{2+} cannot upregulate channels that are already bound to cAMP or 8BrcAMP.

We also asked if Ca^{2+} -mediated I_h upregulation modulated cAMP-dependent effects induced via photolytic release of caged cAMP. We estimated that the maximum cAMP concentration released by a saturating number of flashes (5–20, 10 Hz) corresponds to the relatively low dose of ~ 20 μM cAMP in the patch pipet (not shown). We used only small, nonsaturating numbers of flashes (1–2, corresponding to ~ 4 and ~ 10 μM cAMP, in the patch pipet, respectively) for which flash number and I_h upregulation were linearly related (Fig. 3a and c). After exposure to maximal Ca^{2+} doses (via a saturating volley of hyperpolarizing current injections; Fig. 3b and c), no change in slope was found by linear regression analysis of I_h increase as a function of flash number ($10.6 \pm 1.0\%$ per flash for control; $10.4 \pm 1.5\%$ for upregulated I_h ; $n = 5$; $p > 0.05$), suggesting that I_h enhancement by non-saturating cAMP added linearly to the Ca^{2+} effects (Fig. 3c; $n = 5$). These findings and Fig. 2 demonstrate that effects on I_h are additive at low doses of cAMP and Ca^{2+} , but occlusive at high doses. This supports the hypothesis that I_h upregulation primarily involves cAMP released upon $[\text{Ca}^{2+}]_i$ increases, but not Ca^{2+} -

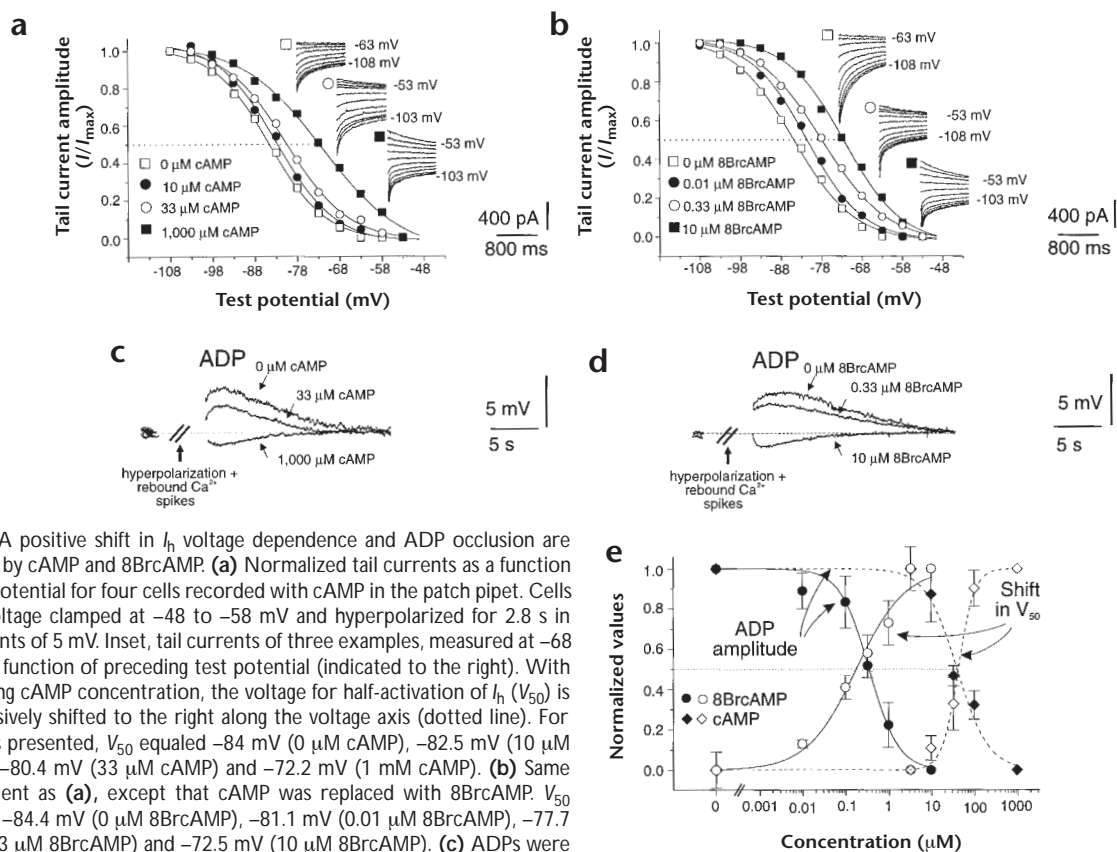


Fig. 2. A positive shift in I_h voltage dependence and ADP occlusion are induced by cAMP and 8BrcAMP. **(a)** Normalized tail currents as a function of test potential for four cells recorded with cAMP in the patch pipet. Cells were voltage clamped at -48 to -58 mV and hyperpolarized for 2.8 s in increments of 5 mV. Inset, tail currents of three examples, measured at -68 mV as a function of preceding test potential (indicated to the right). With increasing cAMP concentration, the voltage for half-activation of I_h (V_{50}) is progressively shifted to the right along the voltage axis (dotted line). For the cells presented, V_{50} equaled -84 mV (0 μ M cAMP), -82.5 mV (10 μ M cAMP), -80.4 mV (33 μ M cAMP) and -72.2 mV (1 mM cAMP). **(b)** Same experiment as **(a)**, except that cAMP was replaced with 8BrcAMP. V_{50} equaled -84.4 mV (0 μ M 8BrcAMP), -81.1 mV (0.01 μ M 8BrcAMP), -77.7 mV (0.33 μ M 8BrcAMP) and -72.5 mV (10 μ M 8BrcAMP). **(c)** ADPs were occluded dose dependently by cAMP. The size of the current injections was increased with enhanced cAMP concentration (0.5 nA for 0 , 10 and 33 μ M cAMP; 1 nA for 100 and $1,000$ μ M cAMP) to compensate for the cAMP-induced decrease in cellular input resistance and to ensure the generation of a low-threshold Ca^{2+} spike at the end of each pulse. Thus, the ADPs shown represent the maximal obtainable ADPs at a given cAMP concentration. A small afterhyperpolarization is observed when the ADP is completely occluded at $1,000$ μ M (ref. 16). Data are from the same cells as in **(a)**, except for 33 μ M cAMP. **(d)** Same experiment as **(c)** repeated with 8BrcAMP instead of cAMP in the patch pipet. Data are from the cells in panel **(b)**. **(e)** Normalized V_{50} shifts (open symbols) and ADP size (closed symbols) as a function of cAMP (diamonds, dotted lines) and 8BrcAMP (circles, solid lines) concentration, fitted with the Hill equation.

dependent modulation of cAMP binding to h-channels (for example, phosphorylation; see below).

Blocking adenylate cyclase reduces Ca^{2+} effects on I_h

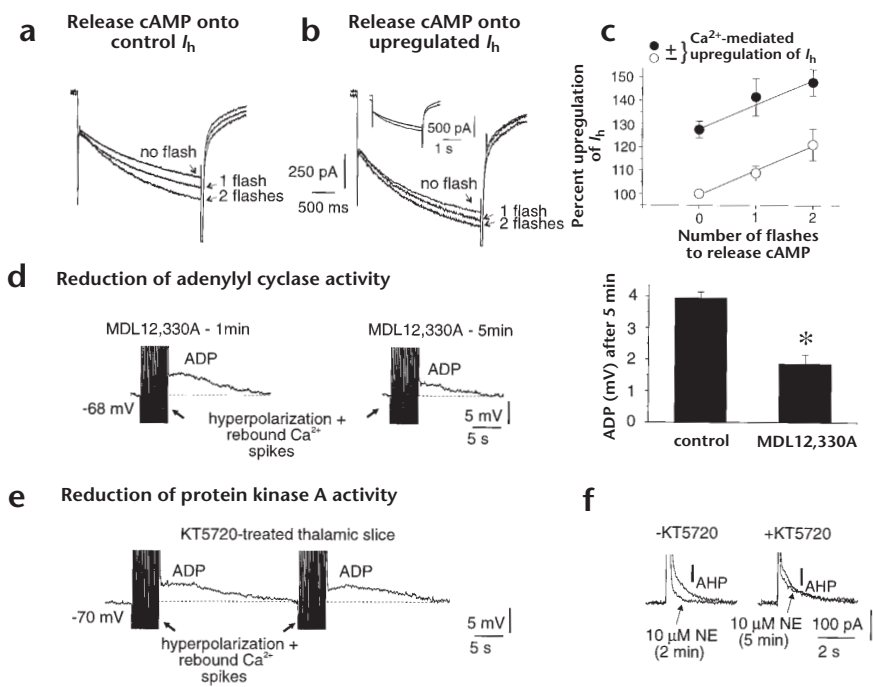
Calcium may enhance I_h by activating a Ca^{2+} -sensitive adenylyl cyclase (AC). This was tested by examining the effects of MDL12,330A, a non-competitive AC inhibitor²⁰ ($\text{IC}_{50} \approx 0.25$ mM; 0.25 – 0.5 mM included in the patch pipet) on ADP generation following a saturating volley of hyperpolarizing current pulses and rebound Ca^{2+} spikes (Fig. 3d). This drug induced a small but significant negative shift of V_{50} for basal I_h activation (from -84.9 ± 1.2 mV, $n = 5$, to -87.7 ± 0.9 mV, $n = 9$; $p < 0.05$, data not shown), suggesting that it inhibited adenylyl cyclase (see Methods). Within 5 minutes of recording with MDL12,330A, ADP amplitude decreased to $47.0 \pm 7.7\%$ of control ($n = 19$; control, 3.9 ± 0.2 mV, $n = 14$; $p < 0.001$). In addition, in 6 of 6 cells perfused with MDL12,330A, flash release of caged Ca^{2+} did not detectably enhance I_h (not shown). Other blockers, such as 2',3'-dideoxyadenosine and SQ 22536, were not used because they induced a positive shift in the activation curve of control I_h (data not shown), probably because of their structural similarity to cyclic nucleotides. These findings support the hypothesis that Ca^{2+} -mediated activation of AC and cAMP release are important for persistent upregulation of I_h .

The h-current may be modulated via phosphorylation through protein kinase A (for review, see ref. 9). To examine this, we incubated thalamic slices with the specific PKA inhibitor KT5720 (5 μ M) for at least two hours²¹ (Fig. 3e). Following incubation, ADPs were not different from those recorded in slices incubated without drug (2.0 ± 0.37 mV, $n = 6$; no drug, 2.3 ± 0.2 mV, $n = 5$; $p > 0.05$). In contrast, the slow afterhyperpolarization current (I_{AHP}) evoked in hippocampal CA1 pyramidal cells incubated simultaneously with the thalamic slices showed a strongly reduced sensitivity to bath application of norepinephrine (Fig. 3f; 10 μ M; $n = 8$ cells in 8 untreated slices; $n = 3$ cells in 3 treated slices). These data suggest that alteration of PKA activity following Ca^{2+} entry is not a primary determinant of Ca^{2+} -mediated upregulation of I_h , and favors a direct interaction of cAMP with the ionic channels underlying I_h , consistent with earlier reports^{9,17}.

Ca^{2+} does not maintain I_h upregulation

To investigate the temporal requirement of Ca^{2+} -dependent I_h enhancement on $[\text{Ca}^{2+}]_i$ increases, we used flash photolysis of the photosensitive buffer diazo-2 (refs. 8, 22). Cells exposed to photolysis-induced release of Ca^{2+} buffer (0.2 – 3 mM in pipet) with a series of flashes of intermediate energy (~ 75 J) showed full blockade of the ADP, similar to the effects of the Ca^{2+} chelator

Fig. 3. Ca^{2+} -mediated I_h upregulation is additive with low doses of cAMP and requires adenylyl cyclase but not PKA activity. **(a)** I_h evoked by a hyperpolarizing step from -53 to -73 mV and exposed to an increasing number of subsaturating UV-flashes (0, 1, 2, traces labeled with arrows) to photolytically release cAMP. I_h amplitude increased when more UV flashes were applied. **(b)** Same cell and protocol as **(a)** except that 20 hyperpolarizing steps were applied to evoke Ca^{2+} -mediated upregulation of I_h before photolytic release of cAMP. Inset, control and Ca^{2+} -induced upregulated currents overlaid; upregulated current is 122.5% of control amplitude. Scale bars apply for **(a)** and **(b)**. **(c)** Percentage increase in I_h amplitude as a function of the number of flashes applied to evoke release of cAMP. All data (**a**, closed circles; **b**, open circles) are normalized to the basal I_h amplitude (trace labeled 'no flash' in **a**). Linear regression coefficient is 0.99 for both fits. **(d)** MDL12,330A (0.5 mM) led to rapid ADP rundown. Pooled data on right ($n = 14$ for control; $n = 19$ for MDL12,330A; $*p < 0.001$). Membrane potential responses to hyperpolarizing current injections are truncated in the hyperpolarizing and depolarizing direction for clearer presentation of the ADP. **(e)** Treatment of slices with KT5720 (5 μM) did not prevent ADP induction. **(f)** In the same experiment, rat hippocampal CA1 neurons treated simultaneously with KT5720 showed greatly reduced sensitivity of the slow AHP current (I_{AHP} , evoked with 100–200 ms, 100 mV depolarizing steps from a holding potential between -50 and -60 mV) to bath application of norepinephrine (NE; 10 μM , racemic).



BAPTA ($n = 4$; data not shown)¹⁶. Higher concentrations of diazo-2 were not used because they evoked rapid, large inward currents, presumably due to blockage of Ca^{2+} -dependent K^+ currents, and led to rundown of basal I_h and Ca^{2+} spikes. In contrast, uncaging of diazo-3 (1 mM), a compound yielding the same photolysis products as diazo-2 (ref. 22) yet not buffering Ca^{2+} , did not reduce ADP amplitude ($n = 3$). The effectiveness of diazo-2 in reducing Ca^{2+} -mediated I_h upregulation allowed us to assess

when increases in $[\text{Ca}^{2+}]_i$ are required for I_h enhancement. Before photolytic release of the Ca^{2+} chelator, cells perfused with diazo-2 showed robust I_h enhancement following repetitive hyperpolarizing current pulses, indicating I_h upregulation by Ca^{2+} (Fig. 4a and b). High-intensity UV flashes (~ 250 J) were then applied either during or after the current injections to buffer Ca^{2+} . Flashes applied immediately after the termination of the hyperpolarizing current injections reduced the extent of upregulation

Fig. 4. Elevated internal free Ca^{2+} concentration is required primarily during induction of Ca^{2+} -mediated I_h upregulation. **(a)** Protocol to study the temporal dynamics of internal free Ca^{2+} during the Ca^{2+} -mediated upregulation of I_h in a cell perfused with 3 mM diazo-2. Twenty large hyperpolarizing current pulses (4 Hz, 125 ms, 1 nA) were applied in current clamp, then we switched to voltage clamp and applied hyperpolarizing steps at times indicated, permitting detection of changes in I_h amplitude. **(b)** H-current amplitudes evoked at the times indicated in **(a)**. Passive current responses were omitted for clarity. Overlay of traces 1 and 5 (right) shows enhancement of I_h amplitude. **(c)** In the same cell, photolytic release of Ca^{2+} buffer immediately after the end of current pulse application induced a moderate (14%) reduction in Ca^{2+} -mediated I_h upregulation. **(d)** Photolytic release of Ca^{2+} buffer at 1 s after onset of current pulse injections led to a strong (86%) reduction in Ca^{2+} -mediated I_h upregulation. **(e)** Partial recovery of Ca^{2+} -mediated I_h upregulation was obtained within ~ 5 min. Some rundown of basal I_h occurred in this experiment (compare traces 5 in **b**–**e**).

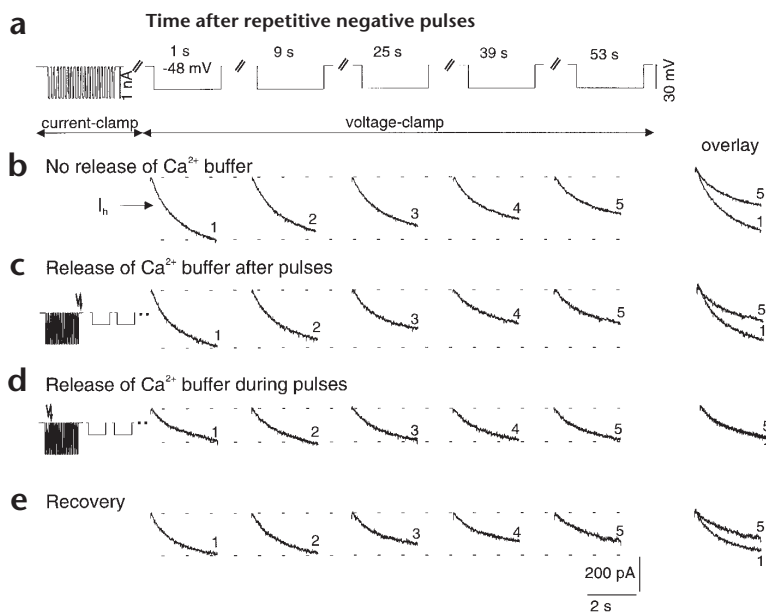
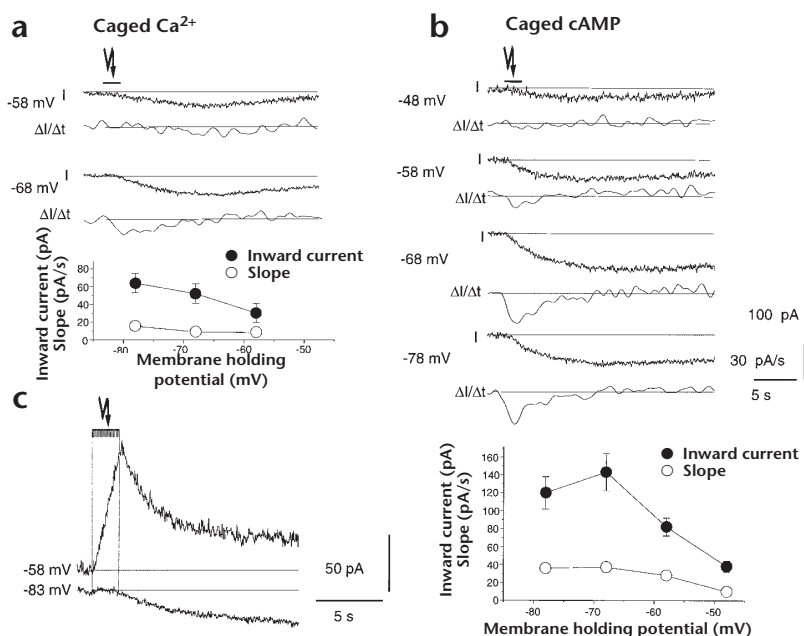


Fig. 5. Photolytic release of Ca^{2+} or cAMP induces inward currents with characteristic slow kinetics. **(a)** Inward currents induced by photolytic release of Ca^{2+} . Their amplitude increased with increasing hyperpolarization, but the initial slope of these inward currents (peak $\Delta I/\Delta t$) increased only moderately. At most, two inward currents per cell could be induced. Error bars are sometimes occluded by the symbols. **(b)** Inward currents induced by photolytic cAMP release, all in the same cell. Amplitude and initial slope (peak $\Delta I/\Delta t$) increased with increasing hyperpolarization and saturated around -70 mV. Calibration bars apply for **(a)** and **(b)**. Error bars are sometimes occluded by the symbols. The time course of the differentiated traces may not perfectly reflect the detailed time course of the change in slope because of smoothing. **(c)** Photolytic release of Ca^{2+} in some cells induced outward currents at more depolarized potentials (-58 mV) due to activation of K^+ currents. These had a short delay (here, ~ 150 ms) and increased along with the application of flashes (arrow, 20 flashes at 10 Hz), in contrast to the slow kinetics of the Ca^{2+} -dependent inward current (-83 mV) recorded in the same cell.



(amplitude ratios for voltage step 1:step 5; **Fig. 4b**) by $27.6 \pm 11.2\%$ (**Fig. 4c**; $n = 5$). In contrast, photolytic release of diazo-2 during current injection was significantly more efficient in compromising the effects of Ca^{2+} on I_h , reducing it by an average of $61.2 \pm 9.8\%$ (**Fig. 4d**; $n = 6$; $p < 0.05$). Partial recovery from this reduction usually occurred within ~ 5 minutes (**Fig. 4e**). The experiments suggest that $[\text{Ca}^{2+}]_i$ increases are primarily required for induction, but not maintenance of I_h upregulation.

Ca^{2+} induces slower inward currents than cAMP

If Ca^{2+} induces cyclic nucleotide release, the kinetics of I_h -dependent inward currents induced by flash photolysis of caged Ca^{2+} should differ from those induced by caged cAMP. Release of Ca^{2+} or cAMP in voltage-clamped cells resulted in slow inward cur-

rents (**Fig. 5**) that increased with hyperpolarizations to approximately -80 mV and were reversibly inhibited 75–100% by Cs^+ ($3\text{--}5$ mM in bath; $n = 4$; data not shown). Current activation kinetics were sigmoidal, with an initial lag followed by a slow rising phase, and were characterized by both the peak slope of the initial downward deflection of holding current ($\Delta I/\Delta t$, lower traces, Methods) and the delay-to-onset of the inward current after a flash. Photolytic release of cAMP triggered inward currents up to ~ 120 pA in amplitude with a peak in $\Delta I/\Delta t$, which increased with increasing hyperpolarization to a maximum of ~ 36 pA/s (**Fig. 5b**). In contrast, Ca^{2+} -induced inward currents were smaller (**Fig. 5a**; $n = 3\text{--}9$ per data point; $p < 0.05$ for all amplitudes) than cAMP currents and had a weakly voltage dependent slope with a maximum of ~ 16 pA/s ($n = 3\text{--}9$ per data

Fig. 6. Voltage gating of I_h stabilizes the interaction with second messenger compounds and therefore causes persistent activation. **(a)** Photolytic release of caged Ca^{2+} (20 flashes at 10 Hz, black bar) transiently enhances I_h amplitude, assessed by repetitively applying hyperpolarizing step commands from -58 to -78 mV (top trace). Right, overlaid traces. In contrast, flash-evoked release of Ca^{2+} while the cell is voltage clamped at a membrane potential that partially activates I_h (-78 mV) induces a slowly developing inward current with substantially slower decay time course (bottom trace). **(b)** Same experiment as **(a)** with photolytic release of cAMP (100 μM in pipet, 20 flashes at 10 Hz, black bar). Again, the duration of the inward current assessed at a holding potential of -68 mV (bottom trace) outlasted the duration of the enhancement detected with voltage steps (top trace). Application of the UV-flash was temporally aligned separately for **(a)** and **(b)**. HP, holding potential.

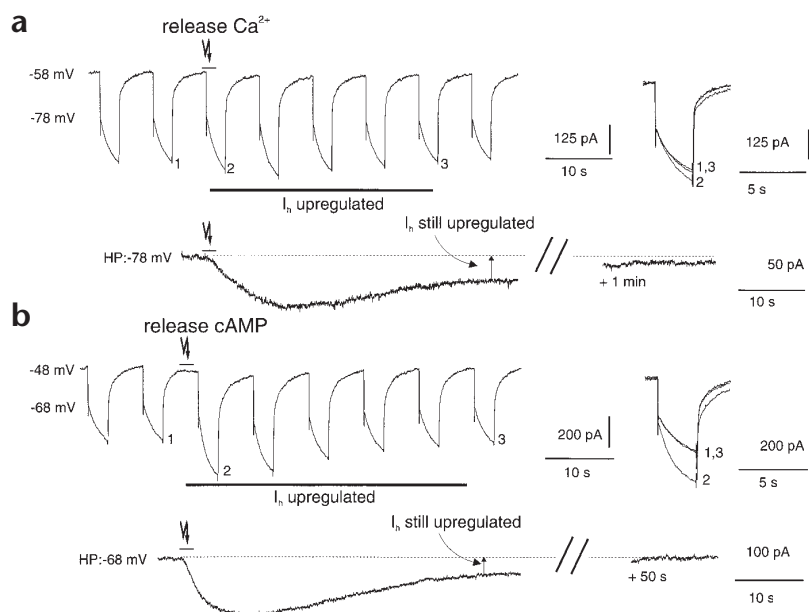
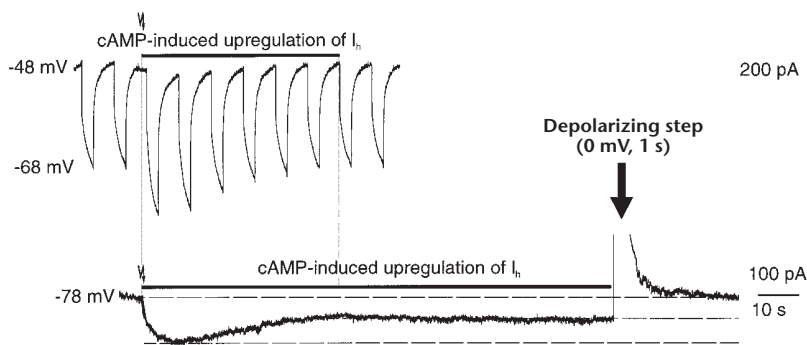


Fig. 7. Depolarizing voltage steps antagonize persistent I_h activation. The cAMP-induced I_h upregulation as detected with step hyperpolarizing voltage commands decayed within ~ 50 s (top). In contrast, the cAMP-induced inward current at -78 mV remained persistent for almost 2 min (bottom). A brief depolarizing step (arrow, response truncated) caused the return of the holding current to levels measured before photolysis.



point; $p < 0.01$ for all values).

Ca^{2+} -induced inward current deflections began 1.23 ± 0.1 seconds ($n = 8$) after the beginning of a flash series ($n = 8$; 15–20 flashes at 10 Hz), whereas cAMP currents showed a significantly shorter lag of 0.25 ± 0.03 seconds ($n = 6$; $p < 0.001$). The onset kinetics of Ca^{2+} -induced inward currents are thus ~ 5 times slower than those of cAMP-induced currents. However, Ca^{2+} diffusion may be slowed because of endogenous Ca^{2+} buffering capacities. We therefore recorded outward currents evoked by photolytic release of Ca^{2+} in cells clamped at potentials at which I_h activation was minimal (-40 to -60 mV). These currents were associated with an increase in input conductance and were voltage dependent (enhanced by depolarization, data not shown), indicating that they were mediated by Ca^{2+} -dependent K^+ conductances²³. Some cells showed both outward currents resulting from K^+ current activation and inward currents resulting from I_h upregulation (Fig. 5c; $n = 7$). The former developed rapidly after flash exposure (delay 0.1–0.2 s, $n = 6$), indicating that $[Ca^{2+}]_i$ rose quickly and thus buffered diffusion was not rate limiting in the gradual I_h upregulation. Therefore, despite rapid $[Ca^{2+}]_i$ increases, Ca^{2+} -triggered I_h upregulation requires more or slower steps than those associated with UV-flash-evoked cAMP release.

I_h voltage gating stabilizes cAMP interaction

The slow time course of the ADP may result from enhanced interaction of activated h-channels with cAMP, for example, via an allosteric mechanism. To test this, we examined the development of I_h enhancement either while the cell was only transiently stepped into the activation range of I_h , or when the cell was held constantly within this range (Fig. 6). Flash photolysis of caged Ca^{2+} or caged cAMP while the cells were stepped repetitively (0.1–0.14 Hz) to voltages between -68 and -88 mV from holding potentials between -48 and -58 mV to transiently activate I_h caused enhancements ($114.0 \pm 2.2\%$, $n = 11$; $p < 0.001$; $141.0 \pm 8.7\%$, $n = 5$; $p < 0.01$) that lasted 53.6 ± 5.3 and 61.0 ± 8.7 seconds, respectively (Fig. 6a and b; durations not significantly different; $p > 0.05$). Cells were then voltage-clamped at a potential corresponding to that reached during the step pulses to partially but constantly activate I_h (Fig. 6a and b). Flash release of Ca^{2+} or cAMP under these circumstances caused the slow development of inward currents that decayed but did not return fully to baseline, even after their effects on I_h had completely reversed as measured by hyperpolarizing steps (see also Fig. 7). Inward currents induced by release of cAMP at potentials below -70 mV persisted for at least 100 seconds and often lasted for 2 or more minutes without full recovery ($n = 8$; $p < 0.05$ compared to duration measured with steps), whereas those induced with release of Ca^{2+} persisted for at least 60 seconds and up to 100 seconds ($n = 8$; $p < 0.01$ compared to duration measured with steps). The

steady-state holding current (measured when the upregulation detected with steps had recovered) equaled 30–60% ($n = 6$) and 30–100% ($n = 8$) of peak inward current amplitude for cAMP and Ca^{2+} , respectively. Thus, the duration of I_h upregulation by Ca^{2+} or cAMP increased with the extent of I_h voltage-gating (see also Fig. 5) and indicated a facilitated interaction between open channels and the upregulating compounds.

Depolarization reverses I_h upregulation by cAMP

If I_h voltage-gating facilitates interaction of cAMP with h-channels, then their closure by depolarization should antagonize the cAMP-mediated effects on I_h . Susceptibility to depolarization of cAMP-mediated I_h upregulation was therefore investigated^{12,16} (Fig. 7). Depolarizing voltage steps (20–80 mV, 1–20 s) were applied to inward currents induced via photolytic release of cAMP. When transient I_h responses had recovered to their control amplitudes but cAMP-induced inward current was still present, these steps gave partial to complete (50–100%) reversal of the holding current levels to pre-flash values in 10 of 15 cells tested ($n = 15$; $p < 0.001$). The sensitivity of cAMP-induced currents to the depolarizing steps varied between cells, probably because of space-clamp variability, and therefore could not be quantified systematically. Overall, depolarizations of 60–80 mV lasting 1–4 seconds yielded full reversal, whereas depolarizations of 20–30 mV lasting up to 20 seconds were only partly effective. Thus, forced deactivation of persistently activated I_h may antagonize the effects of cAMP.

DISCUSSION

Here we studied temporal dynamics of Ca^{2+} -mediated modulation of I_h through flash photolysis of caged compounds. This method allowed us to assess the time course of $[Ca^{2+}]_i$ elevation and to study the kinetics of enzymatic release of second messengers and their interactions with ionic channels in intact cells. We propose that persistent I_h activation is established in thalamocortical cells via Ca^{2+} -stimulated release of cAMP and stabilization of the open h-channel/cAMP complex. The ensuing persistence of the macroscopic current I_h in the activated state seems not to be dependent on maintained increases in $[Ca^{2+}]_i$. Ca^{2+} -mediated upregulation of this current thus represents a 'short-term cellular memory' of the thalamocortical cell's activity that may contribute to the temporal organization of thalamic network function¹⁴. A similar role for I_h has also been proposed in developing hippocampus²⁴ and inferior olive²⁵, suggesting that our study links activity-mediated modulation of single-cell pacemaker currents and a variety of rhythmic network behaviors¹⁰. Moreover, persistent activation of dendritically expressed I_h in CA1 hippocampal pyramidal neurons may contribute to sustained modifications of synaptic integration.

Time course of Ca²⁺ effects on I_h

Rebound Ca²⁺ spikes are characteristic of thalamocortical cells. The low-threshold, voltage-gated Ca²⁺ currents that underlie these Ca²⁺ spikes are strongly expressed on the cellular membrane²⁷, and rebound Ca²⁺ spikes rapidly elevate somatic and dendritic [Ca²⁺]_i, as verified by imaging²⁸. Our results suggest that rises in [Ca²⁺]_i, presumably induced primarily by low-threshold Ca²⁺ currents^{13,16,28}, trigger but are not required to maintain I_h enhancement. Photolytic release of the Ca²⁺ buffer diazo-2 in CA1 pyramidal cells rapidly reduces (within ms) Ca²⁺-activated K⁺ current⁸. In contrast, activation of diazo-2 in thalamocortical neurons could reduce enhancement of I_h primarily during the generation of rebound Ca²⁺ spikes, showing that this enhancement becomes largely Ca²⁺ independent a few seconds after the hyperpolarizing pulses. This suggests that I_h enhancement by [Ca²⁺]_i increases is mediated by an intermediary such as cAMP.

Mechanism of action of [Ca²⁺]_i increases on I_h

Our results strongly suggest that Ca²⁺-mediated stimulation of AC activity²⁹ is important in upregulating I_h. Thus, the shift of I_h voltage dependence and ADP occlusion following repetitive hyperpolarizing current pulses and rebound Ca²⁺ spikes shared a reciprocal dose dependence on cAMP and 8BrcAMP, indicating that Ca²⁺ and the cyclic nucleotides converge onto a common modulatory mechanism. The Hill coefficient of ~1 (measured most accurately by using 8BrcAMP) indicates a 1:1 stoichiometry of binding of cAMP to h-channels, as proposed¹⁷. The reciprocal relationship between the shift in V₅₀ and ADP occlusion demonstrates that the fraction of cAMP-bound h-channels becomes inaccessible to the effects mediated by Ca²⁺, and that cooperative interactions within this cAMP-induced occlusion process are unlikely.

Co-exposure of I_h first to Ca²⁺ and then to non-saturating doses of cAMP revealed an additivity of these two modulatory effects at low doses, but no change in the sensitivity to cAMP (see also ref. 30). This finding, along with the block of Ca²⁺ enhancement of I_h with an adenylyl cyclase antagonist, supports the hypothesis that I_h modulation by Ca²⁺ entry occurs by Ca²⁺-triggered stimulation of cAMP release, most likely via an AC. Alternatively, Ca²⁺ could modulate the levels of cAMP by altering phosphodiesterase activity³¹.

Compared to currents induced by direct cAMP release, Ca²⁺-induced inward currents have approximately fivefold longer delays to onset and twofold slower activation kinetics, indicating that the time required for substantial enzymatic cAMP production is rate limiting. Delay for the Ca²⁺-induced inward currents (~1.2 s) is consistent with that for upregulation measured with repetitive current injections in microelectrode experiments^{13,16} (~1 s) and with *in-vitro* assays⁵ of AC activity stimulated by Ca²⁺/calmodulin. Ca²⁺-sensitive ACs thus activate slowly upon rapid accumulation of intracellular Ca²⁺. To date, nine Ca²⁺-dependent ACs have been described, two of which (AC1 and 8) are stimulated by elevations of [Ca²⁺]_i within physiological ranges²⁹. Type I AC mRNA is expressed in developing rat thalamus³², and this subtype may be targeted by Ca²⁺ entry during synchronized thalamic network activity.

Biophysical properties of I_h

Channel subunits encoding brain-specific forms of I_h have been cloned and termed HCN channels (for hyperpolarization-activated, cyclic-nucleotide-gated channels)^{33,34}. These members of the voltage-gated ion channel superfamily contain a cyclic-

nucleotide binding domain in their carboxy terminus. Our characterization of native currents in thalamocortical cells agrees with the properties of heterologously expressed HCN2 channels, including high sensitivity to cAMP/8BrcAMP and slow kinetics of activation³³. Photolytic release of Ca²⁺ and cAMP now show an as-yet-unidentified channel property permitting persistent upregulation of macroscopic I_h following voltage-dependent activation in conjunction with cAMP release, suggesting preferential binding of cAMP to the open state. Voltage-dependent closure of h-channels may then reverse this persistent upregulation by accelerating unbinding of cAMP from the cyclic-nucleotide-binding domain. Interestingly, spontaneous openings of the molecularly related cyclic nucleotide-gated channels are associated with increased affinity for cyclic nucleotides, presumably via an allosteric gating mechanism^{35,36}. We thus propose that the facilitated interaction of cAMP with open h-channels may reflect allosteric coupling between the voltage-gated closed–open transition and exposure of a high-affinity ligand binding site. These state-dependent interactions between modulatory compounds and channels may also underlie the observed positive shift in the activation curve of the cAMP-induced current with unchanged maximal conductance^{9,11,17,18,37}. Similarly, G-protein-mediated inhibition of voltage-gated Ca²⁺ currents is sensitive to the gating state of the channel and shifts the activation curve of these currents³⁸.

We hypothesize that the coincidence detection of electrophysiological events (hyperpolarization) and biochemical changes in the cellular interior (increases in [cAMP]_i) could underlie the contribution of I_h to the slow periodicity of thalamocortical rhythms during sleep or the re-occurrence of generalized epileptic seizures. Repetitive IPSPs impinging onto thalamocortical cells may lead to partial voltage gating of h-channels and activation of rebound low-threshold Ca²⁺ spikes, resulting in h-channels becoming 'trapped in the open state' by concomitantly released cAMP. This suggests a range in time courses of organization of rhythmic neuronal circuit behavior, from the immediate gating of ionic channels and their modulation by second messenger signals to prolonged alterations in synaptic or cellular properties that produce persistent changes in network behavior. Understanding the details of these interactions may lead to potential targets for therapeutic neurological intervention in sleep disorders and, perhaps, epilepsy³⁹.

METHODS

Electrophysiology and data analysis. Ferrets, 6–7 weeks old, were deeply anesthetized with sodium pentobarbital (30 mg per kg intraperitoneally) and decapitated. Sagittal slices (300–400 μm thick) of the dorsal lateral geniculate nucleus were maintained in a chamber continuously superfused with a solution¹⁵ containing 126 mM NaCl, 2.5 mM KCl, 1.2 mM MgSO₄, 1.25 mM NaH₂PO₄, 2 mM CaCl₂, 26 mM NaHCO₃, 10 mM dextrose. Solutions were aerated with 95% O₂, 5% CO₂ to pH 7.4. Whole-cell patch-clamp electrodes were pulled on a Narishige PP-83 puller and contained 110 mM Kgluconate, 10 mM KCl, 10 mM HEPES, 2 mM MgCl₂, 2 mM Na₂ATP, 0.2 mM NaGTP, 290 mOsm, pH, 7.25. For recordings from rat (2–4 weeks old) hippocampal CA1 cells, gluconate was replaced by MeSO₄ to enhance the outward current amplitude underlying the slow AHP. ATP and GTP were freshly added daily from stock (100-fold concentrated). Calmodulin (20 μM) was added to the pipet solution when studying Ca²⁺ effects on I_h, as this stabilized the upregulation (data not shown). Electrode resistances were 2–3 MΩ and yielded series resistances of 5–12 MΩ that were electronically compensated by 32–80% and checked for stability regularly during the experiments. Particular care for changes in series resistance was applied for slow inward currents induced by flash photolysis of Ca²⁺. A liquid junction potential of 8 mV measured as described⁴⁰ was taken into account for all the data.

Thalamocortical cells were visualized with infrared DIC optics using an upright Axioscope (Zeiss, Germany). Data were collected through an Axopatch-1D amplifier and a multi-channel encoding device (Neurodata Instruments), and stored on videotape for off-line analysis. Data were analyzed with an IBM Pentium computer using pClamp6 software. For differentiation (Fig. 5), Δt was 40 ms, corresponding to the sampling interval, and traces were smoothed. Origin software (Version 4.1) and paired or unpaired *t*-tests were used for data fits and statistical analysis. Norepinephrine was prepared fresh daily as a 1000-fold concentrated solution and kept on ice to prevent oxidation. Data are presented as means \pm s.e.

Photolysis of caged compounds. Flash photolysis of caged Ca^{2+} , caged cAMP and diazo-2 was usually achieved by applying UV flashes within 5–10 min after gaining whole-cell access. For flash photolysis of caged Ca^{2+} , 10 mM DM-Nitrophen (40% Ca^{2+} -loaded) was added to a 280 mOsm solution (Mg^{2+} free). Caged cAMP (100 μM , maximally soluble concentration) was added from a 100-fold concentrated stock solution in DMSO. Separate control experiments showed no effect of 1% DMSO alone on I_h or the Ca^{2+} or cAMP effects on this current. When up to two flashes at different time points per experiment were applied, the sequence was varied to randomize the decreased ability of current injections to upregulate I_h due to prior flash-induced release of Ca^{2+} buffer. The Rapp flashlamp (JML-C1 from HiTech Scientific, UK) delivered single 1 ms UV flashes and was used for the diazo-2 experiments. The Micropoint flashlamp (Photonic Instruments, Arlington Heights) delivered repetitive (5–10 Hz, $\sim 6 \mu\text{s}$) flashes and was used for the caged Ca^{2+} and caged cAMP experiments. Both lamps were attached to the epifluorescence pathway of the microscope. DM-Nitrophen, caged cAMP, calmodulin (bovine brain, high purity), MDL12,330A and KT5720 were from Calbiochem, diazo-2 and diazo-3 from Molecular Probes, norepinephrine from RBI and KMeSO_4 from ICN Biomedicals Inc. All other chemicals were from Sigma.

ACKNOWLEDGEMENTS

The authors thank L. K. Kaczmarek, F. Sigworth, M. V. Sanchez-Vives and J. E. Monckton for discussions and J. C. Brumberg for critically reading the manuscript. A.L. was supported by a Fellowship from the American Epilepsy Foundation. This work was supported by the National Institutes of Health, the McKnight Foundation and the Human Frontier Scientific Program.

RECEIVED 20 JANUARY; ACCEPTED 27 APRIL 1999

- Berridge, M. J. Neuronal calcium signaling. *Neuron* **21**, 13–26 (1998).
- Schulman, H. Protein phosphorylation in neuronal plasticity and gene expression. *Curr. Opin. Neurobiol.* **5**, 375–381 (1995).
- Bading, H., Ginty, D. D. & Greenberg, M. E. Regulation of gene expression in hippocampal neurons by distinct calcium signaling pathways. *Science* **260**, 181–186 (1993).
- Braun, A. P. & Schulman, H. The multifunctional calcium/calmodulin-dependent protein kinase: from form to function. *Annu. Rev. Physiol.* **57**, 417–445 (1995).
- Onyike, C. U., Lin, A. H. & Abrams, T. W. Persistence of the interaction of calmodulin with adenylyl cyclase: implications for integration of transient calcium stimuli. *J. Neurochem.* **71**, 1298–1306 (1998).
- Montminy, M. Transcriptional regulation by cyclic AMP. *Annu. Rev. Biochem.* **66**, 807–822 (1997).
- Jonas, E. A. & Kaczmarek, L. K. Regulation of potassium channels by protein kinases. *Curr. Opin. Neurobiol.* **6**, 318–323 (1996).
- Lancaster, B. & Zucker, R. S. Photolytic manipulation of Ca^{2+} and the time course of slow, Ca^{2+} -activated K^+ current in rat hippocampal neurons. *J. Physiol. (Lond.)* **475**, 229–239 (1994).
- Pape, H.-C. Queer current and pacemaker: the hyperpolarization-activated cation current in neurons. *Annu. Rev. Physiol.* **58**, 299–327 (1996).
- Lüthi, A. & McCormick, D. A. H-current: properties of a neuronal and network pacemaker. *Neuron* **21**, 9–12 (1998).
- McCormick, D. A. & Pape, H.-C. Properties of a hyperpolarization-activated cation current and its role in rhythmic oscillation in thalamic relay neurons. *J. Physiol. (Lond.)* **431**, 291–318 (1990).
- Bal, T. & McCormick, D. A. What stops synchronized thalamocortical oscillations? *Neuron* **17**, 297–308 (1996).
- Lüthi, A., Bal, T. & McCormick, D. A. Periodicity of thalamic oscillations is abolished by ZD7288, a blocker of I_h . *J. Neurophysiol.* **79**, 3284–3289 (1998).
- McCormick, D. A. & Bal, T. Sleep and arousal: thalamocortical mechanisms. *Annu. Rev. Neurosci.* **20**, 185–215 (1997).
- von Krosigk, M., Bal, T. & McCormick, D. A. Cellular mechanisms of a synchronized oscillation in the thalamus. *Science* **261**, 361–364 (1993).
- Lüthi, A. & McCormick, D. A. Periodicity of thalamic synchronized oscillations: the role of Ca^{2+} -mediated upregulation of I_h . *Neuron* **20**, 553–563 (1998).
- DiFrancesco, D. & Tortora, P. Direct activation of cardiac pacemaker channels by intracellular cyclic AMP. *Nature* **351**, 145–147 (1991).
- McCormick, D. A. & Pape, H.-C. Noradrenergic and serotonergic modulation of a hyperpolarization-activated cation current in thalamic relay neurons. *J. Physiol. (Lond.)* **431**, 319–342 (1990).
- Budde, T., Biella, G., Munsch, T. & Pape, H.-C. Lack of regulation by intracellular Ca^{2+} of the hyperpolarization-activated cation current in rat thalamic neurons. *J. Physiol. (Lond.)* **503**, 79–85 (1997).
- Guellaen, G., Mahu, J.-L., Mavier, P., Berthelot, P. & Hanoune, J. RMI 12330 A, an inhibitor of adenylyl cyclase in rat liver. *Biochim. Biophys. Acta* **484**, 465–475 (1977).
- Barajas-López, C. Adenosine reduces the potassium conductance of guinea pig submucosal plexus neurons by activating protein kinase A. *Pflugers Arch.* **424**, 410–415 (1993).
- Adams, S. R., Kao, J. P. & Tsien, R. Y. Biologically useful chelators that take up Ca^{2+} upon illumination. *J. Am. Chem. Soc.* **111**, 7957–7968 (1989).
- Sah, P. Ca^{2+} -activated K^+ currents in neurons: types, physiological roles and modulation. *Trends Neurosci.* **19**, 150–154 (1996).
- Strata, F. *et al.* A pacemaker current in dye-coupled hilar interneurons contributes to the generation of giant GABAergic potentials in developing hippocampus. *J. Neurosci.* **17**, 1435–1446 (1997).
- Bal, T. & McCormick, D. A. Synchronized oscillations in the inferior olive are controlled by the hyperpolarization-activated cation current I_h . *J. Neurophysiol.* **77**, 3145–3156 (1997).
- Magee, J. C. Dendritic hyperpolarization-activated currents modify the integrative properties of hippocampal CA1 pyramidal neurons. *J. Neurosci.* **18**, 7613–7624 (1998).
- Huguenard, J. R. Low-threshold calcium currents in central nervous system neurons. *Annu. Rev. Physiol.* **58**, 329–348 (1996).
- Munsch, T., Budde, T. & Pape, H.-C. Voltage-activated intracellular calcium transients in thalamic relay cells and interneurons. *Neuroreport* **8**, 2411–2418 (1997).
- Cooper, D. M., Karpen, J. W., Fagan, K. A. & Mons, N. E. Ca^{2+} -sensitive adenylyl cyclases. *Adv. Second Messenger Phosphoprotein Res.* **32**, 23–51 (1998).
- Sodickson, D. L. & Bean, B. P. Neurotransmitter activation of inwardly rectifying potassium current in dissociated hippocampal CA3 neurons: interactions among multiple receptors. *J. Neurosci.* **18**, 8153–8162 (1998).
- Beavo J. A. Cyclic nucleotide phosphodiesterases: Functional implications of multiple isoforms. *Physiol. Rev.* **75**, 725–748 (1995).
- Matsuoka, I., Suzuki, Y., Defer, N., Nakanishi, H. & Hanoune, J. Differential expression of type I, II, and V adenylyl cyclase gene in the postnatal developing rat brain. *J. Neurochem.* **68**, 498–506 (1997).
- Ludwig, A., Zong, X., Jeglitsch, M., Hofmann, F. & Biel, M. A family of hyperpolarization-activated mammalian cation channels. *Nature* **393**, 587–591 (1998).
- Santoro, B. *et al.* Identification of a gene encoding a hyperpolarization-activated pacemaker channel of brain. *Cell* **93**, 717–729 (1998).
- Li, J., Zagotta, W. N. & Lester, H. A. Cyclic nucleotide-gated channels: structural basis of ligand efficacy and allosteric modulation. *Q. Rev. Biophys.* **30**, 177–193 (1997).
- Tibbs, G. R., Goulding, E. H. & Siegelbaum, S. A. Allosteric activation and tuning of ligand efficacy in cyclic-nucleotide-gated channels. *Nature* **386**, 612–615 (1997).
- DiFrancesco, D. Dual allosteric modulation of pacemaker (f) channels by cAMP and voltage in rabbit SA node. *J. Physiol. (Lond.)* **515**, 367–376 (1999).
- Bean, B. P. Neurotransmitter inhibition of neuronal calcium currents by changes in channel voltage dependence. *Nature* **340**, 153–156 (1989).
- Steriade, M. in *Generalized Epilepsy. Neurobiological Approaches* (eds Avoli, M. *et al.*) 161–180 (Birkhauser, Boston, 1990).
- Neher, E. Correction for liquid junction potentials in patch clamp experiments. *Methods Enzymol.* **207**, 123–131 (1992).